Icarus 205 (2010) 53–63

Contents lists available at ScienceDirect

Icarus

journal homepage: www.elsevier.com/locate/icarus

HiRISE views enigmatic deposits in the Sirenum Fossae region of Mars

John A. Grant [a,*], Sharon A. Wilson [a], Eldar Noe Dobrea [b], Robin L. Fergason [c], Jennifer L. Griffes [d], Jeffery M. Moore [e], Alan D. Howard [f]

[a] Center for Earth and Planetary Studies, National Air and Space Museum, Smithsonian Institution, Washington, DC 20560, USA
[b] Jet Propulsion Laboratory, California Institute of Technology, Pasadena, CA 91109, USA
[c] United States Geologic Survey, Flagstaff, AZ 86001-1698, USA
[d] Geological and Planetary Sciences, California Institute of Technology, Pasadena, CA 91125, USA
[e] NASA Ames Research Center, Moffett Field, CA 94035, USA
[f] Department of Environmental Sciences, University of Virginia, Charlottesville, VA 22904-4123, USA

ARTICLE INFO

Article history:
Received 7 November 2008
Revised 23 April 2009
Accepted 24 April 2009
Available online 9 May 2009

Keywords:
Mars
Geological processes

ABSTRACT

HiRISE images together with other recent orbital data from Mars define new characteristics of enigmatic Hesperian-aged deposits in Sirenum Fossae that are mostly 100–200 m thick, drape kilometers of relief, and often display generally low relief surfaces. New characteristics of the deposits, previously mapped as the "Electris deposits," include local detection of meter-scale beds that show truncating relationships, a generally light-toned nature, and a variably blocky, weakly indurated appearance. Boulders shed by erosion of the deposits are readily broken down and contribute little to talus. Thermal inertia values for the deposits are ~200 J m^{-2} K^{-1} $s^{-1/2}$ and they may incorporate hydrated minerals derived from weathering of basalt. The deposits do not contain anomalous amounts of water or water ice. Deflation may dominate degradation of the deposits over time and points to an inventory of fine-grained sediment. Together with constraints imposed by the regional setting on formation processes, these newly resolved characteristics are most consistent with an eolian origin as a loess-like deposit comprised of redistributed and somewhat altered volcanic ash. Constituent sediments may be derived from airfall ash deposits in the Tharsis region. An origin directly related to airfall ash or similar volcanic materials is less probable and emplacement by alluvial/fluvial, impact, lacustrine, or relict polar processes is even less likely.

Published by Elsevier Inc.

1. Introduction

The Sirenum Fossae region of Mars contains broadly distributed, unconformable deposits (Fig. 1) mostly from 30°S to 45°S and from 160°E to 200°E (Grant and Schultz, 1990). These deposits, previously mapped as and hereafter referred to by the informal name "Electris deposits," variably mantle ridged plains and cratered upland surfaces (Grant and Schultz, 1990), but the margins do not align well with geomorphic units defined from Mariner 9 data (De Hon, 1977; Howard, 1979). Nevertheless, the morphology and distribution of the materials led previous workers to conclude that eolian processes played a role in emplacement of at least some of the materials (De Hon, 1977; Howard, 1979; Scott and Tanaka, 1986; Greeley and Guest, 1987; Grant and Schultz, 1990). Because the deposits correlate with widespread geomorphic activity elsewhere on Mars (Grant and Schultz, 1990), understanding the processes responsible for their emplacement and modification provides insight into past climatic conditions and geomorphic processes on the planet.

New images from the High Resolution Imaging Science Experiment (HiRISE) (Fig. 1) on the Mars Reconnaissance Orbiter (MRO) (McEwen et al., 2007) together with evaluation of data sets from the Compact Reconnaissance Imaging Spectrometer for Mars (CRISM) on MRO (Murchie et al., 2007) and the Thermal Emission Imaging System (THEMIS) (Christensen et al., 2004; Fergason et al., 2006) and Gamma Ray Spectrometer (GRS) (Feldman et al., 2004) on Mars Odyssey allow a more detailed investigation of the deposits and their characteristics, thereby enabling a reassessment of possible origin.

2. Occurrence and characteristics

Outcrops of the Electris deposits (Figs. 1 and 2) have been well mapped over more than 1.8×10^6 km^2 (Grant and Schultz, 1990), though apparently stripped surfaces south of the present deposits suggest they were once more widespread (Grant and Schultz, 1990). Initial mapping of the region suggested the ages of surfaces including the Electris deposits were as old as the early to mid-Noa-

* Corresponding author. Fax: +1 202 786 2566.
E-mail addresses: grantj@si.edu (J.A. Grant), purdys@si.edu (S.A. Wilson), eldar@caltech.edu (E. Noe Dobrea), rfergason@usgs.gov (R.L. Fergason), griffes@gps.caltech.edu (J.L. Griffes), jeff.moore@nasa.gov (J.M. Moore), ah6p@virginia.edu (A.D. Howard).

0019-1035/$ - see front matter Published by Elsevier Inc.
doi:10.1016/j.icarus.2009.04.009

Fig. 1. THEMIS daytime infrared image mosaic (black areas are gaps in data coverage) from 30°S to 50°S and from 160°E to 210°E covering the approximate mapped extent of the Electris deposits in Sirenum Fossae (Grant and Schultz, 1990). The approximate locations of the center of each primary science phase (PSP) HiRISE image (circles) available for this study (as of June, 2008) are shown, including many images that were reviewed but not used (black circles) because they show surfaces covered by an extensive debris mantle (Mustard et al., 2001), surfaces not covered and/or stripped of deposits (e.g., ridged plains, see Fig. 2), or chaos-like ("Type 4") surfaces. Also shown are locations of HiRISE images used to characterize the Electris deposits in this study (white circles) and those used in figures (labeled, white circles with black dot). The locations of Figs. 2 and 13 are also shown. Illumination from the upper left.

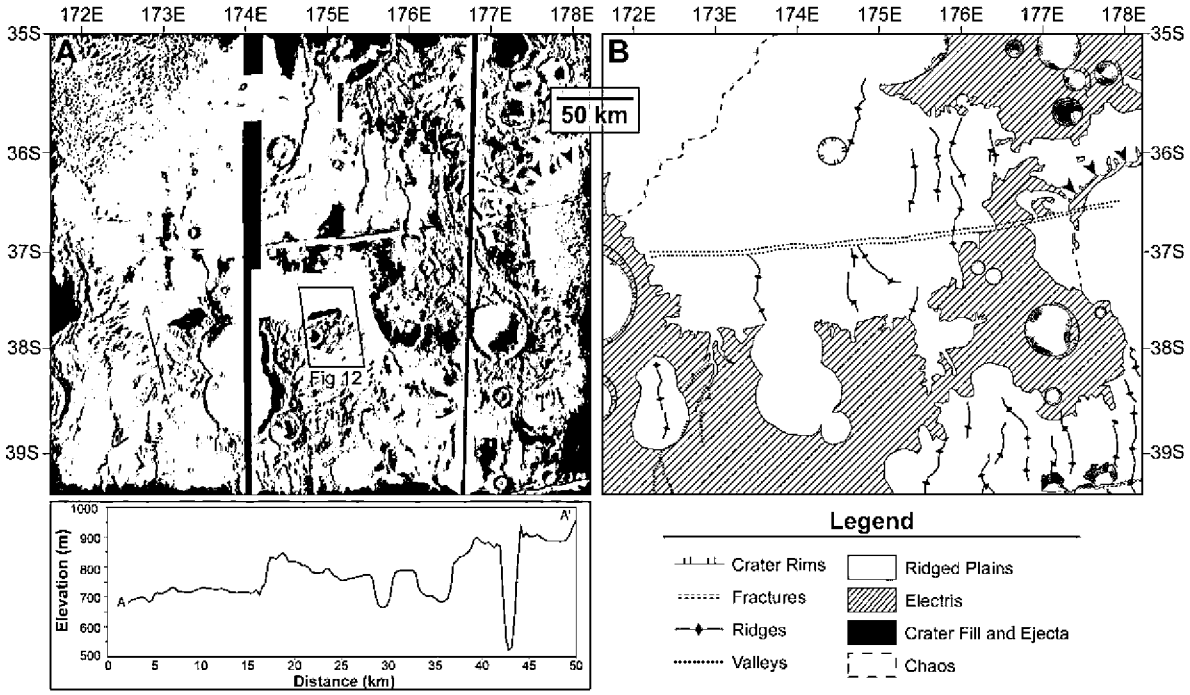

Fig. 2. THEMIS daytime infrared image mosaic (A) and geomorphic map (B) detailing the distribution of a portion of the Electris deposits mapped as "Type 3" and Type 2" (black arrow heads) in Grant and Schultz (1990), underlying ridged plains, and younger chaotic-like ("Type 4" in Grant and Schultz (1990)) materials centered on approximately 37.5°S, 175°E (mosaic covers approximately from 35°S to 39°S and from 172°E to 178°E, see Fig. 1 for context). MOLA data reveal that the thickness of the deposits in this location ranges between ~150 and 200 m (profile A–A′) where valleys appear to have incised to the level of the underlying ridged plains below the deposits. A comprehensive map of the deposits can be found in Grant and Schultz (1990). Data in (A) and map in (B) are rotated approximately 9° counterclockwise relative to Fig. 1. North is towards the top and the location of Fig. 12 is indicated. Illumination in (A) is from the left.

chian (Scott and Tanaka, 1986) to as young as the Amazonian (Greeley and Guest, 1987). More recent relative age-dating analyses and evaluation of superposition relationships, however, constrain emplacement and the bulk of subsequent modification to the middle to late Hesperian (Grant and Schultz, 1990). Hence, modification of the deposits likely followed emplacement by no more than hundreds of millions, rather than billions, of years (Grant and Schultz, 1990). Grant and Schultz (1990) mapped four different occurrences of the Electris deposits. The "Type 1," "Type 2," and "Type 3" materials are distinguished largely on the basis of their occurrence and morphology along their margins and include outcrops that: grade gradually from mantled to unmantled areas; form crude "rings" of material around some large, degraded impact basins (Fig. 2); and are often relatively "flat-topped" and display abrupt, steep margins (Fig. 2), respectively (Grant and Schultz, 1990). By contrast, the "Type 4" materials correlate with buttes and mesas comprising a chaos-like material that occurs within Gorgonum Chaos and other regional basins (Grant and Schultz (1990), mapped as "chaos" in Fig. 2). "Type 4" materials differ in appearance from the other Electris materials (Scott, 1982; Lucchitta, 1982; Schultz and Lutz, 1988; Wilhelms and Baldwin, 1988; Grant and Schultz, 1990; Howard and Moore, 2004; Noe Dobrea et al., 2008) and at the HiRISE scale, they are relatively light-toned, and typically lack obvious bedding or display convo-

luted bedding in outcrops (Noe Dobrea et al., 2008). They are usually capped by a more resistant, darker-toned unit that, when breached, often results in extensive erosion of underlying materials. Such morphologic and other spectral differences from outcrops of deposits of "Types 1–3" suggest the "Type 4" deposits are distinct from and overlie the Electris deposits (Noe Dobrea et al., 2008) and are therefore generally excluded from this discussion.

Previous estimates of Electris deposits thickness ranged between 300 and 700 m based on shadow measurements from Viking images (Grant and Schultz, 1990), but orbital data from the Mars Orbiter Laser Altimeter (MOLA) indicate that typical thicknesses are 150–200 m (Fig. 2) and are locally just over 300 m. Based on the MOLA data, the total volume of the deposit likely exceeds 300,000 km^3. Nevertheless, degraded remnants of craters that are missing raised-rims and occasionally display floors that are near the level of adjacent terrain occur in the deposits in some places (e.g., 40.4°S, 167.3°E; 40.5°S, 172.5°E; 36.0°S, 179.3°E; and 33.9°S, 190.1°E). These degraded craters imply vertical erosion occurred in at least some areas and suggest that the deposits were originally thicker (Grant and Schultz, 1990) or that a later sequence of overlying materials was emplaced, impacted, and subsequently removed.

In places, the Electris deposits are blanketed by a thin, but laterally extensive debris mantle (Mustard et al., 2001; Searls et al., 2007), limiting views of stratigraphy to occasional outcrops in crater walls and along margins of the deposits (Fig. 1). Nevertheless, most surfaces possess a TES albedo of 0.12–0.16 (Christensen et al., 2001) and a dust cover index of 0.96–0.99 (Ruff and Christensen, 2002). These surfaces are not dusty by global standards. The deposits are distributed across kilometers of relief and lie mostly between 1 and 3 km relative to the MOLA datum. Outcrops are often fronted by steep, abrupt margins, and are locally incised by valley networks (Figs. 1–3). Electris materials typically appear somewhat lighter-toned than surrounding materials (Fig. 4) and were thought to consist of crude layers up to tens of meters in thickness based on Viking images (Grant and Schultz, 1990). Examination of the stratigraphy in HiRISE images reveals relatively flat-lying bedding on a variety of scales that includes that observed in Viking data, with meter-scale bedding also observed in some outcrops (Figs. 5 and 6). There is typically little color or tonal variation between strata in the HiRISE data and most appear to reflect minor variations in resistance to erosion based upon the changing expression of the layers across outcrops (Fig. 6). Some beds are laterally continuous and can be traced for kilometers across individual images (Fig. 5), whereas other meter-scale beds display truncating relationships and variable expression over tens of meters (Fig. 6).

Fig. 3. Example of valley system incising the Electris deposits (dashed lines mark edge of valley walls) at 43.1°S, 165.8°E (see Fig. 1 for context). Much of the local surface is covered by a thin debris mantle (Mustard et al., 2001), but in this location does not mask subtle details associated with the relict drainage (arrows indicate margins of apparent floodplain, adjacent surfaces extending to the edge of the valley may form older fluvial/alluvial terraces). Portion of HiRISE image PSP_007632_1365_RED with illumination from the upper left. North is toward the top of the image. Illumination from the upper left.

Fig. 4. The relatively light-toned appearance of the Electris materials is revealed in the upper wall and ejecta of a small crater at 34.9°S, 188.5°E (see Fig. 1 for context) that excavated the deposit. The light-toned appearance of the deposits is somewhat patchy (e.g., not obvious on southeast ejecta and on west upper wall of the crater) due to partial cover by dust and a debris mantle (Mustard et al., 2001). Portion of HiRISE false color image PSP_003504_1450_RGB. North is toward the top of the image. Illumination from the upper left.

HiRISE images reveal exposures of the Electris materials to be variably blocky (diameters typically ~1–2 m), though many outcrops appear free of boulders. Observed blocks are distributed across surfaces (Fig. 7) and some appear to be derived from apparently more resistant layers within outcrops (Fig. 8). Interestingly, many slopes bounding blocky outcrops are flanked by relatively little blocky talus and might reflect the downslope movement and destruction of these blocks (Fig. 8). The upper margins of the deposits occasionally express subtle fractures (Fig. 9). At least one crater exposing the deposits appears nearly rimless despite an otherwise relatively pristine appearance (Fig. 10), whereas another crater presents a prominent bench on the crater floor near the base of the deposits (Fig. 11). The Electris deposits are intermediate-toned in THEMIS daytime infrared (IR) data (Fig. 2A) with thermal inertia values of ~200 $J\,m^{-2}\,K^{-1}\,s^{-1/2}$ (range of 185–290 $J\,m^{-2}\,K^{-1}\,s^{-1/2}$), whereas thermal inertia values are closer to ~300 $J\,m^{-2}\,K^{-1}\,s^{-1/2}$ (range of 250–365 $J\,m^{-2}\,K^{-1}\,s^{-1/2}$) for the adjacent ridged plains materials (Fig. 12). The physical properties of the Electris deposits corresponding to the intermediate thermal inertia values could relate to surfaces of well-sorted sub-millimeter-scale particles (i.e., no larger than sand-sized), finer-grained but indurated material (i.e., cemented), or surfaces with a few percentage cover of blocks within a matrix of fines (e.g., Christensen, 1986; Jakosky and Christensen, 1986; Mellon et al., 2000; Fergason

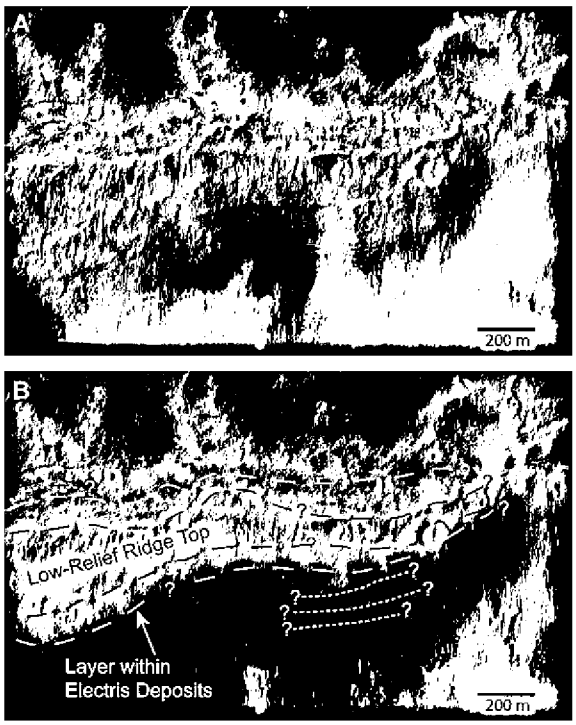

Fig. 5. (A) Subtle layering in an outcrop of the Electris deposits forming a ridge at 36.0°S, 164.2°E (see Fig. 1 for context). (B) Black dashed line defines the relatively flat ridge top and layer extent is identified on the basis of changes in relief and surface roughness. Some individual layers (e.g., white dashed lines) are many meters in thickness and at least one can be traced for kilometers on opposite sides of the ridge. Other layers may also be present (e.g., short white dashed lines on south side of the ridge), but are less easily traced for long distances. Portion of HiRISE image PSP_002094_1435_RED with illumination from upper left. North is toward the top of the image.

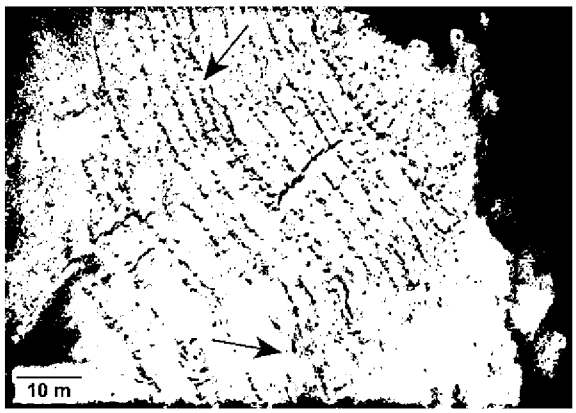

Fig. 6. Meter-scale layering (decreasing in elevation towards the left) in the Electris deposits exposed in a crater wall at 33.9°S, 181.0°E (see Fig. 1 for context). The expression of the layers varies across the crater wall and implies little contrast in strength between them. Some of the layers truncate one another (black arrows) implying that erosion occurred in the time between their emplacement. Portion of HiRISE image PSP_006247_1460_RED. North is toward the top of the image. Illumination from the upper left.

et al., 2006). Although these values correspond to materials within ~10 cm of the surface or less, the differences between the Electris deposits and ridged plains are not likely dominated by the influence of a debris mantle (Mustard et al., 2001). Debris mantle materials occur across both surfaces and more similar thermal inertia values would be expected if the debris mantle was the only material contributing to the thermal inertia values. Hence the debris

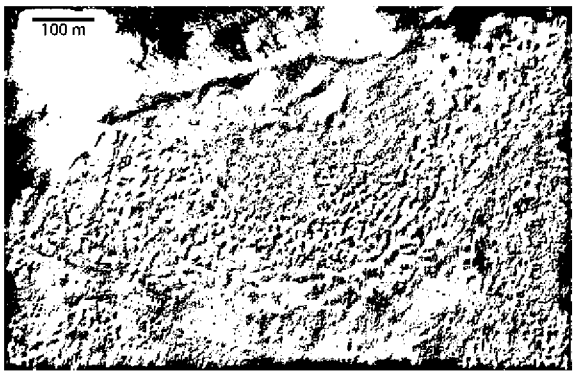

Fig. 7. Local surfaces on the Electris deposits are typically mantled by scattered blocks (40.6°S, 166.9°E, see Fig. 1 for context). Many slopes bounding such blocky surfaces (top of image) are characterized by relatively few large blocks. Portion of HiRISE image PSP_006208_1390_RED. North is toward the top of the image. Illumination from the upper left.

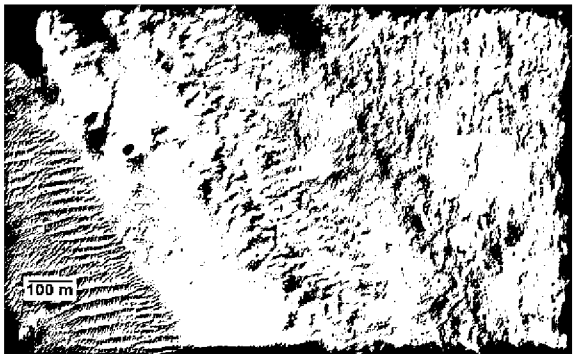

Fig. 8. Outcrop of the Electris deposits (right half of image) exposing apparently rubbly layers that weather into meter-scale blocks on the slopes (37.0°S, 185.4°E, see Fig. 1 for context). Elevation is highest on the relatively flat top of the Electris deposits to the right and slopes down to the left across the outcrop to the dune-mantled surface on the left. The blocks could represent more indurated materials within the outcrop or interbedded layers of impact crater ejecta. Although numerous blocks are present in the outcrop, relatively few occur in the talus near the base of the outcrop, suggesting the blocks are either buried by finer materials and/or broken down quickly and contribute relatively little to the talus. Portion of HiRISE image PSP_001460_1425_RED. North is toward the top of the image. Illumination from the upper left.

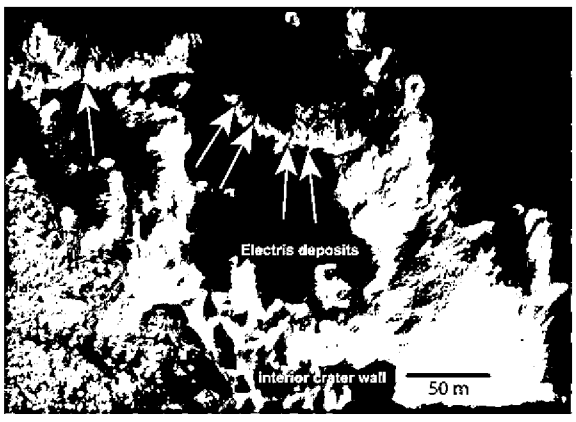

Fig. 9. Subtle fractures (e.g., white arrows) in the Electris deposits along the wall of a crater located at 34.1°S, 209.1°E (see Fig. 1 for context). Note the relatively block free appearance of the Electris materials (above dashed line) relative to knobby underlying substrate exposed in the crater wall (below dashed line). Portion of HiRISE image PSP_007604_1455_RED with illumination from the upper left. North is toward the top of the image.

Fig. 10. The wall and proximal ejecta deposit of a small crater (down is to the right) in Electris at 35.7°S, 180.5°E (see Fig. 1 for context). The apparent lack of a significant raised-rim around the crater may relate to its formation into stratigraphy capped by the Electris deposits. Low strength materials, such as is inferred for the Electris deposits, may result in back wasting of steep slopes along the original crater wall, thereby destroying much of the raised rim. Portion of HiRISE image PSP_008462_1440_RED. North is toward the top of the image. Illumination from the upper left.

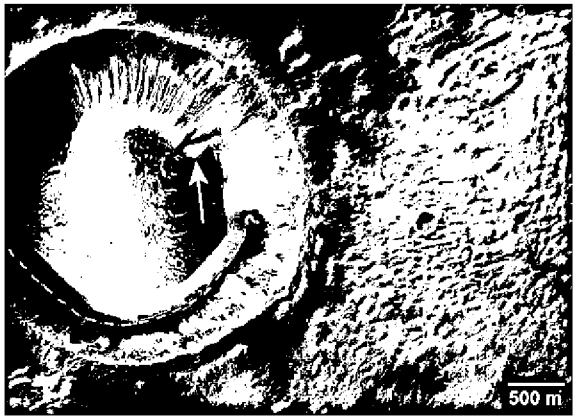

Fig. 11. Prominent bench (dashed line) exposed along the wall of a 3 km-diameter crater at 34.2°S, 165.6°E (see Fig. 1 for context). Impacts into layered targets can produce benches on crater walls (Quaide and Oberbeck, 1968) where weaker materials near the surface, corresponding to the Electris deposits in this location, are removed to a larger diameter than more competent materials at depth. Note the relatively bright appearance of the materials being shed down gullies heading within the weaker materials inferred to represent the Electris deposits (e.g., arrow). Gullies are concentrated on the north or pole facing walls of the crater as is the case for many southern mid-latitude gullies (Dickson et al., 2007). Portion of HiRISE image PSP_004929_1455_RED with illumination from the upper left. North is toward the top of the image.

mantle appears to be no more than a few centimeters thick in many locations in this region. Finally, eolian ripples or transverse eolian ridges are numerous in the vicinity of the Electris deposits (Wilson and Zimbleman, 2004), but dunes and other features that might reflect a large inventory of sand-sized material are not widespread compared to other locations (e.g., western Argyre and western Hellas) in the same general latitude band (Hayward et al., 2007).

3. Composition and water

While the thermal inertia data appears to penetrate the dust and debris mantle in Sirenum Fossae (Mustard et al., 2001), compositional data from CRISM is derived from generally lesser depths and is less successful in sampling the Electris deposits. Compositional information for the deposits is further limited by a general paucity of high resolution CRISM observations. One CRISM observation, HRL000063D1, targets an outlier of the deposits at 35.1°S, 188.6°E, and a spectrum was derived by averaging an area covering 10 × 10 pixels (Fig. 13). The spectrum, albeit noisy, is dominated by a positive, concave-up slope from 1 to 2.2 μm that is interpreted

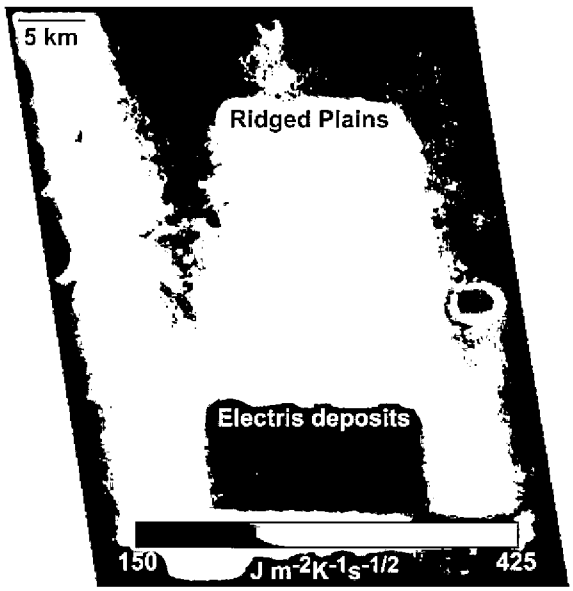

Fig. 12. Thermal inertia for a portion of the Electris deposits and ridged plains derived using THEMIS night time IR image I17250012 (see Fig. 2 for context). The Electris deposits have a thermal inertia of around 200 J m^{-2} K^{-1} s$^{-1/2}$ (range from 185 to 290 J m^{-2} K^{-1} s$^{-1/2}$), whereas the ridged plains possess a thermal inertia closer to 300 J m^{-2} K^{-1} s$^{-1/2}$ (range of from 250 to 365 J m^{-2} K^{-1} s$^{-1/2}$). These thermal inertia values for the deposits are consistent with indurated, fine-grained sediments capped by surfaces partially covered by scattered blocks. Values for the ridged plains are consistent with a rockier surface, perhaps with some exposed bedrock.

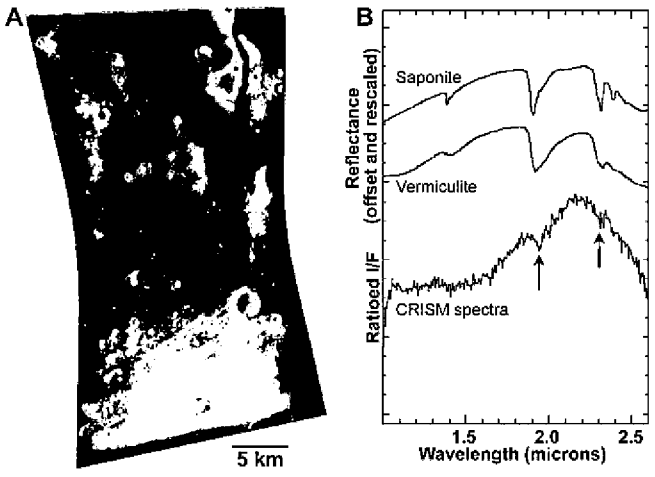

Fig. 13. (A) CRISM image HRL000063D1 RGB (R = 2.53 μm, G = 1.08 μm, B = 1.51 μm) showing variations in mineralogy between outcrops of the Electris deposits (light-toned) and underlying ridged plains materials (reddish tones) near 35.1°S, 188.6°E (see Fig. 1 for context). (B) CRISM spectrum (ratioed I/F) from the Electris deposits averaged from a 10 × 10 pixel area corresponding to the approximate area covered by the black dot on the knob in (A). Comparison mineral spectra in (B) are offset and rescaled for comparison and are from the CRISM spectral library (http://pds-geosciences.wustl.edu/MROCRISMSpectralLibrary/) and correspond to entries CAVE02 (vermiculite) and C1SA53 (saponite). Arrows indicate absorptions in the CRISM spectrum at ~1.9 and ~2.3 μm, which are indicative of hydration and Fe/Mg–OH bonding in phyllosilicates, respectively. North toward the top of (A) and illumination is from the upper left.

to be indicative of a ferrous component. A subtle 1.9 μm feature is also present, likely indicative of hydration (caused by a combination of the H_2O bend overtone with an OH stretch overtone). An additional subtle absorption at about 2.31 μm may relate to a Fe/Mg–OH stretch. Because Fe–OH and Mg–OH stretches usually are located around 2.28 and 2.31 μm, respectively, the absorption may relate to an Mg–OH stretch (the absorption detection is at the 1-sigma level and the noisy nature of the data makes this difficult to confirm). Spectra of saponite (Mg-smectite) and vermiculite (Mg-phyllosilicate) may provide a match for these features (Mustard et al., 2008), but ferrous mica cannot be ruled out. The paucity of environments on Mars associated with the formation of mica suggests that saponite and vermiculite are better candidate minerals for any hydrated phase as both are derived from aqueous alteration of basalt and can contain a range of Fe and Mg ratios in the octahedral sites. Occurrence of a hydrated phase implies the deposits are not comprised of pristine volcanic materials.

Derived water abundance values for Sirenum Fossae from the GRS (Feldman et al., 2004) show broad correlation with the distribution of the Electris deposits and indicate 3–4 wt% of H_2O in the uppermost ~0.5 m of the deposits in many locations, but are closer to 2 wt% in some areas. These values are low relative to the greater than ~50% water abundance characterizing most latitudes north and south of 55° and the ~10% water abundance occurring in regions in Arabia and around Gusev crater and Ma'adim Vallis (Feldman et al., 2004). The uppermost ~0.5 m of the ridged plains occurring stratigraphically below and that are typically exposed adjacent to outcrops of the Electris deposits are also generally deficient in water relative to other parts of Mars and are characterized by 2–3 wt% water. Slightly increased water abundance values in the deposit relative to the plains may be real, but are not high relative to other regions of the planet (Feldman et al., 2004). Ice may be stable in the deposits at greater depths than characterized by both the GRS and thermal inertia data (Paige, 1992). However, the lack of evidence for flow in the deposits or other morphologic evidence for ice, absence of obvious variation in water enrichment across outcrops and ejecta deposits of presumably varying exposure ages, and the paucity of stratigraphy (e.g., bright versus dark layers) that might indicate abundant ice, argue that the bulk of the deposits are not enriched in water or water ice.

4. Implications for the nature of Electris deposits

The process(es) responsible for emplacement of the Electris deposits must be consistent with the observations from all available data sets as summarized in Table 1 and discussed below. Deposition occurred over kilometers of relief, including craters and ridged plains materials and resulted in layered sequences totaling hundreds of meters in thickness. Distinct stratigraphy at a variety of scales (Figs. 5 and 6) requires multiple depositional and/or pedogenic events over some increment of time. The deposits appear distinct from underlying and adjacent materials and possess a generally lighter-toned appearance. They display lower thermal inertia than adjacent ridged plains and possess apparently low internal strength (overall) based on morphology of outcrops, back-wasted crater rims, and benches formed in some craters (Figs. 4, 10 and 11). The presence of meter-scale blocks, both in layers and across surfaces (Figs. 7 and 8), implies varying amounts of induration and/or introduction of blocks from other sources (e.g., nearby impacts). The relative paucity of blocks and talus at the base of many slopes, however, suggests that blocks are efficiently broken down over short travel distances and may not significantly differ in their resistance to erosion from block-free surfaces of the deposits. Lateral variations in the expression of meter-scale beds on the scale of tens of meters and negligible variation in color and tone between layers (Fig. 6) implies that differences between the blocky and block-free horizons are fairly subtle and may not be due to significant differences in composition or induration.

The paucity of blocky talus at the base of many of the steeper outcrops, including along some crater walls (Fig. 8), implies efficient erosion of materials comprising the Electris deposits without formation of extensive remnant lags. Occurrence of considerable erosion is demonstrated by wholesale removal of the deposits in some areas and significant relief within remaining outcrops in other locations. Moreover, steep outcrops that sometimes transect craters indicate that appreciable back wasting has occurred in what are apparently fairly uniform sediments.

Maintenance of steep outcrops during back wasting may require occurrence of a more resistant cap unit or erosion focused near the base of the outcrop (Howard, 1978). Occurrence of a more resistant capping layer may be consistent with the low-relief surface characterizing many occurrences of the deposits (Figs. 1 and 2) that express fractures in a few locations (Fig. 9). Together with the occurrence of degraded remnants of craters, these characteristics may relate to deflation down to a more resistant horizon. A more resistant cap layer is not obviously expressed in outcrops along the deposit margin, however, but it may be difficult to resolve if the layer were very thin or occurred as unconsolidated lag. There is a dearth of morphologies adjacent to the outcrops indicative of fluvial processes capable of eroding and transporting material away from the base of some steep outcrops. Other steep outcrops, however, face basins that may have been occupied by

Table 1
Potential emplacement origins and whether they could potentially satisfy observed morphologic characteristics of the Electris deposits.

Observed morphology	Possible emplacement processes						
	Lava flow	Fluvial	Impact	Lacustrine	Relict polar	Airfall ash	Eolian
Regional setting	No	No	No	No	Maybe	Maybe	Yes
Extent of deposit	Maybe	Maybe	Yes[a]	Yes	Yes	Yes	Yes
Thickness of deposit	Yes	Yes	Yes	Maybe	Yes	Yes	Yes
Range of relief	No	No	Yes	No	Yes	Yes	Yes
Bounding slopes	No	No	Yes	–	Yes	Yes	Yes
Scale of beds	No	Maybe	No	Yes	Yes	Yes	Yes
Extent of beds	Maybe	No	No	No	Maybe	Maybe	Yes
Mostly silt or sand-sized	No	Maybe	No	Yes	Yes	Yes	Yes
Presence of boulders	Yes	Maybe	Yes	No	Maybe	Maybe	Yes
Low strength	No	Maybe	Maybe	Maybe	Maybe	Maybe	Yes
Light-toned	No	Maybe	Maybe	Yes	Maybe	Yes	Yes
Composition	Maybe	Maybe	Maybe	Maybe	Maybe	Yes	Yes
Thermal inertia	No	Maybe	No	Yes	No	Yes	Yes

[a] Although formation of a large impact basin could yield ejecta deposits extending over an area equivalent to that covered by the Electris deposits, no candidate impact basin is present.

lakes (Howard and Moore, 2004) that could have focused erosion at the base of the outcrops while maintaining their steep expression.

Eolian deflation is capable of producing gradational margins crossing a range of relief similar to those characterizing some of the deposits. Deflation can also help break down and remove talus shed from steeper margins, but requires that the deposits consist of, or weather into, fairly uniform, fine-grained sediment. The thermal inertia is consistent with this interpretation and suggests an abundance of silt or fine sand-sized sediment if unconsolidated, but could be mostly silt-sized if the deposit is somewhat indurated and the effects of the scattered blocks found on the deposits are factored in. For comparison, White Rock on Mars (8.0°S, 25.0°E) is likely comprised of indurated, fine-grained sediment or dust and possesses a thermal inertia of 125–185 J m^{-2} K^{-1} $s^{-1/2}$ (Mellon et al., 2008), which is slightly lower than the ~200 J m^{-2} K^{-1} $s^{-1/2}$ thermal inertia value for the Electris deposits. By contrast, thermal inertia values of closer to 300 J m^{-2} K^{-1} $s^{-1/2}$ for the ridged plains (Fig. 12) imply a rockier surface that may include bedrock outcrops (Nowicki and Christensen, 2007). The general paucity of eolian dunes and ripples is consistent with deposits containing abundant silt-sized and smaller material, but it is unclear why yardangs, a landform commonly associated with eolian erosion (Pye, 1987), are uncommon.

Sparse compositional data suggest that the Electris deposits are not comprised of pristine volcanic materials and may include a hydrated phase such as saponite or vermiculite (Fig. 13). GRS data and morphologic and stratigraphic information supports the presence of some limited water within the deposits, but does not point to an unusually high abundance of volatiles. This is indirectly supported by the thermal inertia data which should be a factor of two or more higher if there is a significant fraction of water ice incorporated into the near surface of the deposits (Mellon et al., 2008). Hence, hydrated phases may have formed prior to incorporation into the deposits.

5. Origin of the Electris deposits

A variety of processes have been considered for emplacement of some or all of the Electris deposits including eolian, volcanic, fluvial, and impact (De Hon, 1977; Howard, 1979; Scott and Tanaka, 1986; Greeley and Guest, 1987); lacustrine (Howard and Moore, 2004), relict polar deposits (Schultz and Lutz, 1988), and eolian airfall (Grant and Schultz, 1990; Schultz, 2002; Moore and Howard, 2005). Grant and Schultz (1990), Moore and Howard (2005), and Wilson et al. (2007) provide pre-HiRISE summaries of the relative merits associated with these processes, which are expanded upon below to include constraints imposed by the new data (Table 1). For example, the emplacement process must be consistent with the scale, continuity, and variably blocky stratigraphy seen in HiRISE images and other characteristics that imply a relatively low internal strength (Table 1). The thermal inertia and compositional information place additional constraints on processes responsible for the deposits (Table 1). These newly resolved details confirm that the bulk of the Electris deposits were probably not related to fluvial, volcanic lava, impact, or lacustrine origins (Table 1).

The thermal inertia, presence of some large blocks and composition of the deposits could be consistent with a fluvial origin (Table 1), but does not require it. And although several properties (Table 1) might be consistent with volcanic lava flows, such as the occurrence of large blocks and perhaps composition (if weathered in place), the fine-grained nature of the bulk of the material inferred from patterns of erosion and thermal inertia probably precludes an origin as volcanic lava flows (Table 1). Lava and fluvial deposits might be consistent with the lateral extent of the Electris materials, but the distribution across kilometers of relief coupled with an absence of flow features, observed abrupt bounding slopes, the extent and scale of bedding, and the lack of source vents and basins makes these origins unlikely (Grant and Schultz, 1990; Moore and Howard, 2005; Table 1). There is no volcanic center or broadly integrated system of valleys on or near the deposits. Finally, fluvial deposits would typically show greater variability in expression and grain size due to lateral juxtaposition of depositional environments that is not consistent with the fairly uniform appearance of the Electris deposits (Table 1).

The lateral extent, thickness, occurrence over kilometers of relief, and abrupt bounding slopes of the deposits is consistent with emplacement as ejecta associated with a large basin-forming impact (Table 1). It is also conceivable that ejecta around a large basin could produce a low strength, light-toned deposit with a composition similar to the Electris deposits, though the thermal inertia of a blocky ejecta deposit would be higher than is observed. However, there is no evidence of a large enough and relatively well-preserved basin in the vicinity that could account for the scale of the deposits. Moreover, the scale and extent of bedding, coupled with the generally fine-grained nature of the deposits and the distribution of blocks mostly within beds rather than throughout the deposits likely rule out an origin related to impact processes (Table 1). Nevertheless, impacts probably do contribute to some of the blocks observed in Electris given the large number of smaller craters in the region that post-date the deposits. Emplacement of blocks as ejecta might be most consistent with their discontinuous occurrence on surfaces, but this apparent distribution could also be the result of subsequent debris mantling that obscures a more complete observation of their distribution (Mustard et al., 2001).

Deposition in a large lake is consistent with the lateral extent, inferred fine-grained nature, and scale of some beds in the Electris deposits (Table 1). Lacustrine deposits can also be relatively light-toned and have a thermal inertia comparable to the Electris deposits. Composition, thickness and inferred low strength of the deposits might also be consistent with a lacustrine origin. The presence of numerous, large blocks, especially those occurring in relatively discrete strata, however, cannot easily be accounted for by ice-rafting or incorporation of impact crater ejecta because they appear to be uniformly distributed in some layers, absent from others, and there is no obvious source impact craters or basins. Lacustrine deposits are also inconsistent with the observation that, where observed, the meter-scale beds truncate one another over distances of tens to hundreds of meters. Moreover, the distribution of the deposits does not correspond to any obvious topographic basin and the occurrence of multiple beds shedding blocks may argue against a lacustrine origin. A large lake may once have covered the Eridania region to the northwest and extended across much of the region mantled by the Electris deposits (Irwin et al., 2002). The lake sourced Ma'adim Vallis and was confined to elevations below 1100 m (Irwin et al., 2002). The Electris deposits drape relief well above the level occupied by such a lake and indicate its origin was not related to the Eridania impoundment. It is worth noting that the "Type 4" deposits mapped by Grant and Schultz (1990) does occur within large, degraded impact structures (mapped as "chaos" in Fig. 2) and may be lacustrine (Howard and Moore, 2004). These deposits are younger than the Electris deposits and could represent eroded and redistributed Electris materials.

An airfall origin for the deposits was favored by Grant and Schultz (1990) and Schultz (2002) and was forwarded by Moore and Howard (2005). Although the airfall interpretation for the Electris materials predates data from HiRISE, newly defined properties enable a more robust consideration of the merits of the process than was previously possible. For example, airfall deposition can produce beds whose vertical distribution, thickness, and scale are

consistent with what is observed for some bed in the Electris deposits. Airfall deposition is broadly consistent with emplacement of a regional deposit blanketing kilometers of relief (Grant and Schultz, 1990) and the lack of any large-scale, basin-encompassing topography associated with the deposit. The overall thickness of the deposits, which appear relatively uniform, can also be consistent with some types of airfall processes.

Airfall deposition can include accumulation of atmospheric ice and dust during a past interval of polar wandering (Schultz and Lutz, 1988), emplacement of pyroclastic fragments as airfall ash deposits associated with volcanic activity (Moore and Howard, 2005), or deposition of windblown fines as loess (Pye, 1987). The detailed evaluation of the Electris stratigraphy within the context of the regional setting enables some distinction between these possible origins.

Comparison between the Electris deposits and the present day polar materials reveals significant differences in their nature. Polar deposits are fine-grained and can possess steep bounding slopes, but variable inclusion of ice yields thermal inertias that should be higher in at least some layers than is inferred (Mellon et al., 2008) and layers that might be less uniformly low strength, light-toned, and of more variable composition (Table 1). Individual beds comprising the bulk of polar deposits are probably formed by airfall deposition of varying proportions of ice and dust and yields beds that are more continuous than the intermittent meter-scale stratigraphy seen in the Electris deposits (Howard et al., 1982; Milkovich and Head, 2005; Fishbaugh and Hvidberg, 2006). Although materials forming the basal section of the north polar and some of the south polar deposits display bedding that may be more similar to that observed in Electris in terms of extent and thickness, they are comprised of contrasting beds of ice-rich and more sandy material (Herkenhoff et al., 2007), yielding a sequence that is quite different from the more subtle layered stratigraphy in the Electris deposits. Moreover, GRS, thermal inertia, and morphologic and stratigraphic data for Electris do not suggest abundant ice in the near surface or at depth as might be expected for relict polar materials.

Interestingly, the fine-grained, ice-rich beds of the basal section north polar deposits produce large, meter-scale blocks during back wasting along scarps that appear to disintegrate (either throughout their down slope transport or once they are at the base of the slope), and rarely accumulate to form extensive talus (Herkenhoff et al., 2007). Although production of weak blocks from discrete layers and the apparent under-representation of these blocks in polar talus is a characteristic that may be similar to the Electris deposits, the broader differences between polar and Electris materials implies emplacement in different settings. If the Electris deposits represent relict polar materials, their accumulation was characterized by evolution of beds whose extent, range in expression, and inferred ice content was less than at the present-day Martian poles.

Deposition of volcanic pyroclastic material in the form of airfall ash or tuff is another candidate origin for the Electris deposits (Moore and Howard, 2005). Accumulation of airfall ash can produce a fine-grained, low strength, light-toned mantle over preexisting topography during periods of volcanic activity (Table 1). Erosion occurring between eruptions would be capable of producing the truncations observed between the meter-scale beds, but finer, continuous beds, which might be expected to occur within the meter-scale stratigraphy if they are ash deposits, are not detected (Table 1). Slightly more resistant, apparently blocky layers could reflect erosional lags or materials that are weakly welded (Keszthelyi et al., 2008) and the angular nature of constituent grains could impart the limited strength needed to create abrupt outcrop margins. Alternatively, the more resistant layers could represent pedogenic horizons developed between depositional events (Schultz et al., 1998; Schultz, 2002).

The broad extent and thickness of the Electris deposits coupled with its fairly uniform bulk properties and relatively low thermal inertia imply a large and distant source if they are related to accumulation of pyroclastic materials (Table 1). Putative volcanic constructs proposed for the Electris region (e.g., Scott, 1982; Wilhelms and Baldwin, 1988) appear relatively more degraded than the deposits (and possibly older) and are probably not large enough to be responsible for the deposits. Early effusive activity in the Tharsis region provides another possible source of ash, though more thinning of the deposit from the source and with elevation would be expected than is observed if sediment were being actively transported by prevailing winds (Pye, 1987). A possible airfall ash deposit in Tharsis is distinguished in HiRISE imagery and is relatively light-toned in appearance (Keszthelyi et al., 2008), but appears to lack the truncating, meter-scale beds observed in Electris. If derived directly from Tharsis or any other distant volcanic construct, intervening deposits should be at least as thick as those in Electris but these deposits do not occur (in any form similar to the Electris deposits) and would have to be completely eroded while leaving widespread outcrops of the materials in Electris largely intact. Nevertheless, there are locations within the Electris deposits where the material has been entirely removed (Fig. 2). The limited compositional data for the deposits implies pristine volcanic materials are not present, but that could simply relate to some in situ alteration after emplacement. Collectively, these characteristics are not the best match for a primary pyroclastic origin for the Electris deposits.

Emplacement of the Electris deposits as eolian loess would produce many of the observed broad-scale characteristics of the materials and could represent a variation of a primary volcanic airfall ash origin that is most consistent with the full range of characteristics (Table 1). On the Earth, loess commonly occurs as relatively light-toned regional deposits up to 100–200 m thick, can mantle a range of relief (Pye, 1987), and is formed by the erosion of sediment from a source region that is transported by the wind and deposited in sinks. Like primary ash deposits, loess would accumulate in response to the availability of fine-grained sediment within source areas, as enabled by geomorphic or climatic processes. Terrestrial loess deposits on relatively flat-lying surfaces are of fairly constant thickness, but deposits in the presence of significant relief, perhaps more comparable to the Electris deposits, are of varying thickness and tend to thin with elevation (Pye, 1987). If the Electris deposits are loess, the more uniform thickness that is inferred implies little down slope redistribution during or subsequent to emplacement.

Loess accumulation typically results in unstratified deposits (Pye, 1987) that would be consistent with the absence of continuous, sub-meter beds in Electris (Fig. 6, Table 1). Erosion and pedogenic activity between periods of deposition and accumulation (Schultz et al., 1998; Schultz, 2002) could redistribute material and produce the truncating meter-scale stratigraphy and apparently blocky beds, respectively. Larger-scale, more continuous beds in Electris may reflect master bed sets perhaps controlled by climate change, whereas smaller scale, less continuous beds may record individual epochs of deposition related to changing availability of source materials (Figs. 5 and 6). Accumulation of materials eroded and transported from elsewhere on Mars is consistent with the limited compositional information implying the presence of minor hydrated phases such as saponite or vermiculite in Electris (Fig. 13). These minerals, however, could also be derived via in situ weathering (Table 1).

Terrestrial loess deposits are typically comprised of silt-sized grains 10–50 μm across and possess low to moderate internal strength that commonly results in vertical outcrops (Pye, 1987). The abrupt, steep margins and apparently fine-grained but somewhat indurated nature of the Electris deposits inferred from erosional patterns and thermal inertia data are analogous if capped

by a resistant layer or if later lacustrine or alternate processes focused erosion along the base of outcrops (Table 1). Terrestrial loess deposits sometimes develop tension cracks that are sub-parallel to adjacent steep faces and eventually cause failure and back wasting of outcrops (Pye, 1987). Subtle fractures observed at the top of the Electris deposits are more orthogonal to outcrop faces (Fig. 9) and it is unclear whether they relate to a more resistant near-surface bed and a similar mode of failure and back wasting. While some blocks in the Electris deposits are almost certainly ejecta derived from impacts (Fig. 7), shedding of numerous blocks from layers within outcrops and their rapid breakdown and minimal contribution to talus (Fig. 8) is analogous to what is observed in some terrestrial loess (Fig. 14; Table 1). Slightly more resistant, apparently blocky layers in Electris could correspond to pedogenic horizons, thereby causing their variable expression relative to material in adjacent layers (Fig. 6).

Terrestrial loess often has a high infiltration capacity that limits runoff and can inhibit incision (Pye, 1987). If the meter-scale beds in the Electris deposits (Fig. 6) record pedogenic alteration and concentration/incorporation of clays (Schultz, 2002), as is observed in some loess deposits on the Earth (Schultz et al., 1998, Fig. 14), they would represent weak aquitards capable of laterally deflecting infiltrating water and facilitating incision (Figs. 2 and 3).

Although the valleys incised into the Electris deposits together with other indirect evidence led Grant and Schultz (1990) to suggest the deposit was volatile-rich, the GRS and thermal inertia data along with a lack of morphologic or stratigraphic evidence for water/ice or deformation/flow may not support this interpretation. These GRS, thermal inertia, morphologic, and stratigraphic data imply any hydrated phase noted in the CRISM data may have formed prior to incorporation into the deposits. Loess deposits on the Earth likely owe their competence at least in part to binding by clays that can be diminished when saturated, leading to slumping or collapse (Pye, 1987). Therefore, if the Electris deposits are analogous to loess, abundant liquid water could reduce internal strength and lead to flow which is not observed. Abundant water might also preclude the abrupt, steep bounding slopes and fractured margins of the deposits that are observed. Hence, the valleys incising the Electris deposits may reflect incision in response to post-deposition availability of at least some water derived from regional or global sources rather than saturation or drainage from extensive sources within the deposits that might preclude the often steep expression of outcrops.

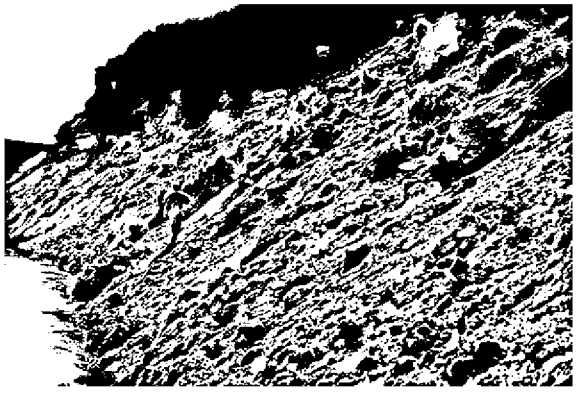

Fig. 14. Loessoid deposits exposed via fluvial incision in the vicinity of Rio Cuarto, Argentina. Outcrops in these and other loess deposits often maintain steep to vertical faces and shed large blocks during back wasting such as those in the upper-right portion of the image. Blocks often represent slightly more indurated material and break down quickly during downslope transport and contribute little to the flanking talus. Blocks often occur along pedogenically altered horizons which are responsible for producing the meter-scale stratigraphy visible in the outcrop (top). If the Electris deposits are loess, blocks and meter-scale stratigraphy may have similar origins. Photo taken by first author, note person for scale.

6. Source of sediments

Origin of the Electris deposits as loess may be most consistent with the suite of observed and inferred characteristics. An origin as airfall ash or other primary pyroclastic deposits is less favored due to the lack of an obvious nearby source. More distant candidate sources (e.g., Tharsis or volcanic centers to the north and west) require wholesale removal of intervening material while preserving the Electris deposits. Moreover, deposits comparable to those in Electris are not widespread around Tharsis or other distant volcanic centers, and the expression of one inferred airfall ash deposit in Tharsis (Keszthelyi et al., 2008) differs from what is observed in Electris. Deposits formed by other volcanic, fluvial, impact, lacustrine, or polar processes are even less likely to possess the range of observed characteristics (Table 1).

If the Electris deposits are loess, their emplacement reflects eolian transport and deposition of fines deflated from distant source regions. On the Earth, source regions can include a variety of settings that include alluvial, periglacial, and volcanic (Pye, 1987; Schultz et al., 1998), where sediment inventories are often influenced by multiple geomorphic processes (Pye, 1987). On Mars, potential processes capable of producing large inventories of fine sediment include alluvial, periglacial, seasonal precipitation and condensation at the poles, impact and volcanic. Widespread valley formation on Mars predates the Electris deposits (Carr, 1996) and comparable deposits are not associated with valleys elsewhere, thereby suggesting either their complete erosion or that alternate sources supplied sediment to the Electris deposits. Deflation of sediments from ancient periglacial or polar layered terrains provides other potential sediment sources, but it is unclear why deposits comparable to those in Electris are not detected in the northern hemisphere unless they did exist but were completely eroded. A fourth potential source of sediment is ejecta deposits around large impact craters. Although large craters and basins have formed at a declining rate across Mars history, there are no obvious candidate ejecta deposits that would serve as a source of the Electris deposits and it is unclear why similar deposits would not have formed in association with multiple basin forming impacts elsewhere unless they were also formed and subsequently completely eroded. In addition, analysis of ejecta deposits around small impact craters on the Earth and Mars indicates that minimal erosion of ejecta produces armored surfaces resistant to additional erosion (Grant and Schultz, 1993; Grant et al., 2006, 2008), thereby suggesting that the inventory of fines available for deflation around large craters may not be large. A fifth source of sediment includes ash related to volcanic activity at Tharsis or other volcanic centers. Although the bulk of the Tharsis rise predates the Electris deposits (Phillips et al., 2001), post-Noachian lava flows mantle almost the entire surface of Tharsis Montes (Carr, 2006) and were likely emplaced during episodic intervals of activity (Wilson and Head, 2001). Although large scale volcanic landforms are widespread on Mars (Carr, 2006), events responsible for construction of the Tharsis volcanoes probably represent the largest potential inventory of ash that is broadly coeval with the emplacement of the Electris deposits. If correct, each major episode of activity at Tharsis could yield fine-grained ash deposits available for deflation and transport to Sirenum Fossae. The large scale, more continuous stratigraphy in the Electris deposits would represent accumulation during major eruptive phases versus individual eruptions and/or short-term climate driven changes responsible for meter-scale beds. Pedogenic alteration and deflation between intervals of

accumulation could yield slightly more resistant beds and beds showing truncating relationships.

Although the source(s) of the sediment comprising the Electris deposits cannot be positively identified, it appears that volcanic materials in the Tharsis region or perhaps another volcanic center are leading candidates. Hence, the distinction between origins of the deposits as primary airfall ash versus loess may be subtle, relating primarily to transport to Sirenum Fossae subsequent to initial deposition and any in situ weathering that occurred closer to Tharsis or elsewhere.

It is unclear why mostly eolian erosion of the Electris deposits would lead to complete removal in some locations while adjacent regions preserve a more uniform thickness and abrupt bounding slopes. On the Earth (Fig. 14), fluvial incision of loess creates steep bluffs that maintain slopes well above the angle of repose (Pye, 1987). In Sirenum Fossae, the past occurrence of valleys (Figs. 1 and 2) or lakes (Howard and Moore, 2004) may have eroded large areas and created outcrop relief that was subsequently modified by deflation and slope retreat, but never led to widespread saturation of the deposits.

7. Conclusions

HiRISE images and data from other instruments orbiting Mars define new characteristics of the Electris deposits in the Sirenum Fossae region. These characteristics place additional constraints on their origin which remains most consistent with eolian airfall (Grant and Schultz, 1990; Schultz, 2002; Moore and Howard, 2005). These characteristics, in concert with the regional setting and occurrence of the deposits, suggest that accumulation as loess is most likely. Sediments forming the deposits may have been derived from volcanic materials in Tharsis or another volcanic center and provides the most consistency between the observed and expected morphology and stratigraphy. An origin associated with primary deposition of ash is less likely. It is even less likely that the deposits represent accumulation of ancient polar materials, lava, alluvial/fluvial, impact, or lacustrine sediments. If the Electris deposits are loess, their distribution may help constrain sediment transport processes and prevailing winds during the Middle to Late Hesperian period on Mars.

Acknowledgments

We thank the people at the University of Arizona, Ball Aerospace, the Jet Propulsion Laboratory, and Lockheed Martin that built and operate the HiRISE camera and the Mars Reconnaissance Orbiter Spacecraft. Reviews by Kevin Williams, Ken Herkenhoff, and an anonymous reviewer improved the manuscript. This work was supported by NASA.

References

Carr, M.H., 1996. Water on Mars. Oxford University Press, New York.
Carr, M.H., 2006. The Surface of Mars. Cambridge University Press, New York.
Christensen, P.R., 1986. The spatial distribution of rocks on Mars. Icarus 68, 217–238.
Christensen, P.R.and 25 colleagues, 2001. Mars Global Surveyor Thermal Emission Spectrometer experiment: Investigation description and surface science results. J. Geophys. Res. 106 (E10), 23823–23871.
Christensen, P.R.and 10 colleagues, 2004. The Thermal Emission Imaging System (THEMIS) for the Mars 2001 Odyssey Mission. Space Sci. Rev. 110, 85–130.
De Hon, R.A., 1977. Geologic map of the Eridania quadrangle of Mars. U.S. Geol. Survey Misc. Invest. Series Map I-1008.
Dickson, J.L., Head, J.W., Kreslavsky, M., 2007. Martian gullies in the southern mid-latitudes of Mars: Evidence for climate-controlled formation of young fluvial features based upon local and global topography. Icarus 188, 315–323.
Feldman, W.C.and 14 colleagues, 2004. Global distribution of near-surface hydrogen on Mars. J. Geophys. Res. 109. doi:10.1029/2003JE002160.
Fergason, R.L., Christensen, P.R., Kieffer, H.H., 2006. High resolution thermal inertia derived from THEMIS: Thermal model and applications. J. Geophys. Res. 111, E12004. doi:10.1029/2006JE002735.
Fishbaugh, K., Hvidberg, C., 2006. Martian north polar layered deposits stratigraphy: Implications for accumulation rates and flow. J. Geophys. Res. 111 (E06012). doi:10.1029/2005JE002571.
Grant, J.A.and 10 colleagues, 2008. Degradational modification of Victoria crater, Mars. J. Geophys. Res. 113. doi:10.1029/2008JE003155.
Grant, J.A., Schultz, P.H., 1990. Gradational epochs on Mars: Evidence from west-northwest of Isidis Basin and Electris. Icarus 84, 166–195.
Grant, J.A., Schultz, P.H., 1993. Erosion of ejecta at Meteor Crater, Arizona. J. Geophys. Res. 98, 15033–15047.
Grant, J.A., Arvidson, R., Crumpler, L.S., Golombek, M.P., Hahn, B., Haldemann, A.F.C., Li, R., Soderblom, L.A., Squyres, S.W., Wright, S.P., Watters, W.A., 2006. Crater gradation in Gusev crater and Meridiani Planum, Mars. J. Geophys. Res. 111. doi:10.1029/2005JE002465.
Greeley, R., Guest, J.E., 1987. Geologic map of the eastern equatorial region of Mars. U.S. Geol. Survey Misc. Invest. Series Map I-1802-B.
Hayward, R.K., Mullins, K.F., Fenton, L.K., Tutus, T.N., Bourke, M.C., Colaprete, T., Hare, T., Christensen, P.R., 2007. Mars digital dune database: Progress and application. Lunar Planet. Sci. 37, 1360. Abstract.
Herkenhoff, K.E., Byrne, S., Russell, P.S., Fishbaugh, K.E., McEwen, A.S., 2007. Meter-scale morphology of the North Polar Region of Mars. Science 317, 1711–1715. doi:10.1126/science.1143544.
Howard, A.D., 1978. Origin of the stepped topography of the martian poles. Icarus 34, 591–599.
Howard III, J.H., 1979. Geologic map of the Phaethontis quadrangle of Mars. U.S. Geol. Survey Misc. Invest. Series Map I-1145.
Howard, A.D., Moore, J.M., 2004. Scarp-bounded benches in Gorgonum Chaos, Mars: Formed beneath and ice-covered lake? Geophys. Res. Lett. 31. doi:10.1029/2003GL018925.
Howard, A., Cutts, J., Blasius, K., 1982. Stratigraphic relationships within the martian polar cap deposits. Icarus 50, 161–215.
Irwin III, R.P., Maxwell, T.A., Howard, A.D., Craddock, R.A., Leverington, D.W., 2002. A large Paleolake Basin at the head of Ma'adim Vallis, Mars. Science 296, 2209–2212.
Jakosky, B.M., Christensen, P.R., 1986. Global duricrust on Mars: Analysis of remote-sensing data. J. Geophys. Res. 91, 3547–3559.
Keszthelyi, L., Jaeger, W., McEwen, A., Tornabene, L., Beyer, R.A., Dundas, C., Milazzo, M., 2008. High resolution imaging science experiment (HiRISE) images of volcanic terrains from the first 6 months of the Mars Reconnaissance Orbiter Primary Science Phase. J. Geophys. Res. 113, E04005. doi:10.1029/2007JE002968.
Lucchitta, B.K., 1982. Preferential development of chaotic terrains on sedimentary deposits, Mars. NASA technical memorandum 85127, 235–236.
McEwen, A.S.and 14 colleagues, 2007. Mars Reconnaissance Orbiter's High Resolution Imaging Science Experiment (HiRISE). J. Geophys. Res. 112, E05S02. doi:10.1029/2005JE002605.
Mellon, M.T., Jakosky, B.M., Kieffer, H.H., Christensen, P.R., 2000. High resolution thermal inertia mapping from the Mars Global Surveyor Thermal Emission Spectrometer. Icarus 148, 437–455.
Mellon, M.T., Fergason, R.L., Putzig, N.A., 2008. The thermal inertia of the surface of Mars. In: Bell, J.F. (Ed.), The Martian Surface: Composition, Mineralogy, and Physical Properties. Cambridge University Press, Cambridge, pp. 399–427.
Milkovich, S., Head, J., 2005. North polar cap of Mars: Polar layered deposit characterization and identification of a fundamental climate signal. J. Geophys. Res. 110 (E05). doi:10.1029/2004JE002349.
Moore, J.M., Howard, A.D., 2005. Layered deposits and pitted terrain in the circum Hellas region. Lunar Planet. Sci. 36, 1512. Abstract.
Murchie, S.and 49 colleagues, 2007. Compact Reconnaissance Imaging Spectrometer for Mars (CRISM) on Mars Reconnaissance Orbiter (MRO). J. Geophys. Res. 112, E05S03. doi:10.1029/2006JE002682.
Mustard, J.F.and 35 colleagues, 2008. Hydrated silicate minerals on Mars observed by the Mars Reconnaissance Orbiter CRISM instrument. Nature 454, 305–309. doi:10.1038/nature07097.
Mustard, J.F., Cooper, C.D., Rifkin, M.K., 2001. Evidence for recent climate change on Mars from the identification of youthful near-surface ground ice. Nature 412, 411–413.
Noe Dobrea, E.Z., Moore, J., Howard, A., Catling, D., Grant, J.A., 2008. Spectral and geomorphic evidence for a past inland sea in Eridania Basin, Mars. Eos [Fall Suppl] 89, P32B-03. Abstract.
Nowicki, S.A., Christensen, P.R., 2007. Rock abundance of Mars from the thermal emission spectrometer. J. Geophys. Res. 112, E05007. doi:10.1029/2006JE002798.
Paige, D.A., 1992. The thermal stability of near-surface ground ice on Mars. Nature 356, 43–45. doi:10.1038/35604a0.
Phillips, R.J.and 10 colleagues, 2001. Ancient geodynamics and global-scale hydrology on Mars. Science 291, 2587–2591.
Pye, K., 1987. Aeolian Dust and Dust Deposits. Academic Press, London, UK.
Quaide, W.L., Oberbeck, V.R., 1968. Thickness determination of the lunar surface layer from impact craters. J. Geophys. Res. 73, 5247–5270.
Ruff, S.W., Christensen, P.R., 2002. Bright and dark regions on Mars: Particle size and mineralogical characteristics based on Thermal Emission Spectrometer data. J. Geophys. Res. 107. doi:10.1029/2001JE001580.
Schultz, P.H., 2002. Uncovering Mars. Lunar Planet. Sci. 33, 1790. Abstract.
Schultz, P.H., Lutz, A.B., 1988. Polar wandering of Mars. Icarus 73, 91–141.

Schultz, P.H., Zarate, M., Camilion, C., King, J., 1998. A 3.3-Ma impact in Argentina and possible consequences. Science 282, 2061–2063. doi:10.1126/science.282.5396.2061.

Scott, D.H., 1982. Volcanoes and volcanic provinces: Martian western hemisphere. J. Geophys. Res. 87, 9839–9851.

Scott, D.H., Tanaka, K.L., 1986. Geologic map of the western equatorial region of Mars. U.S. Geol. Survey Misc. Invest. Series Map I-1802-A.

Searls, M.L., Mellon, M.T., Mustard, J.F., Milliken, R.E., Martinez-Alonso, S., HiRISE Team, 2007. Mid-latitude dissected mantle terrain as viewed from HiRISE. In: Proceedings of the Seventh International Conference on Mars, Abstract 3351.

Wilhelms, D.E., Baldwin, R.J., 1988. The role of igneous sills in shaping the martian uplands. Lunar Planet. Sci. 19, 1270–1271. Abstract.

Wilson, L., Head, J.W., 2001. Evidence for episodicity in the magma supply to the large Tharsis volcanoes. J. Geophys. Res. 106, 1423–1433.

Wilson, S.A., Zimbleman, J.R., 2004. Latitude-dependent nature and physical characteristics of transverse aeolian ridges on Mars. J. Geophys. Res. 109, E10003. doi:10.1029/2004JE002247.

Wilson, S.A., Howard, A.D., Moore, J.M., Grant, J.A., 2007. Geomorphic and stratigraphic analysis of Crater Terby and layered deposits north of Hellas basin, Mars. J. Geophys. Res. 112, E08009. doi:10.1029/2006JE002830.